SANDIA REPORT

SAND2015-11101
Unlimited Release
Printed October 2015

Inversion for Eigenvalues and Modes using SIERRA-SD and ROL

Timothy Walsh, Wilkins Aquino, Denis Ridzal, Drew Kouri

Prepared by
Sandia National Laboratories
Albuquerque, New Mexico 87185 and Livermore, California 94550

Sandia National Laboratories is a multi-program laboratory managed and operated by Sandia Corporation, a wholly owned subsidiary of Lockheed Martin Corporation, for the U.S. Department of Energy's National Nuclear Security Administration under contract DE-AC04-94AL85000.

Sandia National Laboratories

Issued by Sandia National Laboratories, operated for the United States Department of Energy by Sandia Corporation.

Available to DOE and DOE contractors from
U.S. Department of Energy
Office of Scientific and Technical Information
P.O. Box 62
Oak Ridge, TN 37831

Telephone: (865) 576-8401
Facsimile: (865) 576-5728
E-Mail: reports@adonis.osti.gov
Online ordering: http://www.osti.gov/bridge

Available to the public from
U.S. Department of Commerce
National Technical Information Service
5285 Port Royal Rd
Springfield, VA 22161

Telephone: (800) 553-6847
Facsimile: (703) 605-6900
E-Mail: orders@ntis.fedworld.gov
Online ordering: http://www.ntis.gov/help/ordermethods.asp?loc=7-4-0#online

SAND2015-11101
Unlimited Release
Printed October 2015

Inversion for Eigenvalues and Modes using SIERRA-SD and ROL

Timothy Walsh
Computational Solid Mechanics and Structural Dynamics
Sandia National Laboratories
P.O. Box 5800
Albuquerque, NM 87185-0845
tfwalsh@sandia.gov

Wilkins Aquino
Department of Civil and Environmental Engineering
Pratt School of Engineering
Duke University
Box 90287
121 Hudson Hall
Durham, NC 27708-0287

Denis Ridzal, Drew Kouri
Optimization and Uncertainty Quantification
Sandia National Laboratories
P.O. Box 5800
Albuquerque, NM 87185-1320

Abstract

In this report we formulate eigenvalue-based methods for model calibration using a PDE-constrained optimization framework. We derive the abstract optimization operators from first principles and implement these methods using Sierra-SD and the Rapid Optimization Library (ROL). To demonstrate this approach, we use experimental measurements and an inverse solution to compute the joint and elastic foam properties of a low-fidelity unit (LFU) model.

Contents

List of Figures

List of Tables

This page intentionally left blank.

Introduction

Predicting material properties from experimental measurements is a pervasive need in engineering systems, and spans multiple physics such as elasticity and viscoelasticity[15,3,4] as well as thermal analysis, and electromagnetics.[16] Material inversion is a systematic methodology for reconstructing the missing material parameters from direct experimental measurements. Traditionally, Sandia has relied on modal tests to calibrate finite element models. Thus, in this report we derive an operator-based optimization approach that is based on an eigenvalue formulation.

The literature contains a wealth of references that deal with the subject of *inverse eigenvalue problems*.[5,6] Many of these methods seek to find entries in the stiffness or damping matrix such that a set of spectral data is matched. As such, there is no direct connection between these methods and standard parameters in a finite element model. In this work we take an alternative approach in that the parameters in the optimization process are chosen to correspond directly to physical material parameters of interest. These parameters then have a direct link to the finite element model.

Parameter estimation in structural dynamics has a long history at Sandia. The PEGA[17] and PESTDY[7] software packages used genetic algorithms and a gradient-based strategy, respectively, to compute parameters in structural dynamics models. More recently, the ATTUNE[9] software has been used in conjunction with Sierra-SD to calibrate structural dynamics models.

In this report we describe an operator-based PDE-constrained optimization approach to eigenvalue-based model calibration. One advantage of this approach is that it allows most of the software to be re-used for other types of inverse problems, such as associated with transient analysis and direct frequency response. In addition, this approach allows us to leverage Sandia-developed optimization software that provides a rich set of algorithms for solving large-scale simulation-constrained optimization problems. This software also provides capabilities to handle bound constraints on the parameters, which has been found to be critical for success of the model calibration. Results along these lines will be demonstrated later in the report.

We also highlight the need for design variable scaling and bound constraints in the optimization procedure. The former converts the design variables to dimensionless quantities that have comparable magnitudes. This mitigates the case where different parameters have vastly different magnitudes, which can cause numerical difficulties in the optimization algorithms. In addition, bound constraints prevent unrealistic design variable iterates (e.g. negative moduli) which can lead to failures either in the optimization or in the linear solver. The benefits of these features are demonstrated in the numerical examples.

Once the optimization operators are defined, we derive the objective function and gradient operations that are used to interface with the optimization solver. These methods have been implemented in the Sierra-SD(Structural-Dynamics) framework,[1,18] leveraging much of the same infrastructure that was recently developed for force identification[22] and material identification.[21] The objective function, gradient, and Hessian operations directly interface with the Rapid Optimization Library (ROL)[13] which is used to solve the optimization problem. ROL is Trilinos[10]

package for large-scale optimization. It is used for the solution of optimal design, optimal control and inverse problems in large-scale engineering applications.

We note that problems with repeated or crossing eigenvalues can present difficulties in the context of derivative-based optimization, due to non-differentiability of the eigenvalues and eigenvectors as functions of material properties.[20, 19, 8] We do not address these issues now as they will be a subject of an additional report.

This report is organized as follows. First, we provide formulations for the forward problems of interest. Then, we cast the inverse problem as PDE-constrained optimization problem. We derive the abstract optimization operators for eigenvalue problems and provide details for the efficient computation of gradients using an adjoint-based approach. We then present numerical results of material inversion study using both synthetic and experimental data on a low-fidelity unit (LFU) model.

Eigenvalue Problem

In the case of a linear structure, the discretized eigenvalue problem is to find the first l eigenvalues, $\lambda_i, i = 1,\ldots,l$, and eigenvectors $\boldsymbol{u}_i \in \mathbb{R}^m, i = 1,\ldots,l$, such that $l \leq m$ and

$$\boldsymbol{K}\boldsymbol{u}_i = \lambda_i \boldsymbol{M}\boldsymbol{u}_i \tag{1}$$

where $\boldsymbol{K} \in \mathbb{R}^m \times \mathbb{R}^m$ is the stiffness matrix, $\boldsymbol{M} \in \mathbb{R}^m \times \mathbb{R}^m$ is the mass matrix, $\boldsymbol{u} = \{\boldsymbol{u}_i\} \in \mathbb{R}^k$ are the eigenvectors, $k = m \times l$ is the product of the dimension of the stiffness matrix and the number of modes, and $\boldsymbol{\lambda} = \{\lambda_i\} \in \mathbb{R}^l$ is a vector containing the eigenvalues.

We define a discretized PDE operator $\boldsymbol{g}(\boldsymbol{u}, \boldsymbol{\lambda}, \boldsymbol{p}) = \boldsymbol{g}(\{\boldsymbol{u}_i\}, \{\lambda_i\}, \boldsymbol{p}) = \{\boldsymbol{g}_i\}$ as

$$\boldsymbol{g}_i = \boldsymbol{g}(\boldsymbol{u}_i, \lambda_i, \boldsymbol{p}) = \boldsymbol{K}(\boldsymbol{p})\boldsymbol{u}_i - \lambda_i \boldsymbol{M}\boldsymbol{u}_i, \qquad i = 1,\ldots,l. \tag{2}$$

Note we are only considering parameters that effect the stiffness matrix, and not the mass matrix.

When solving the forward eigenvalue problem (1), the eigenvectors $\boldsymbol{u}_i$ can be scaled by any arbitrary factor. We choose to work with mass-normalized eigenvectors, and thus we consider the additional constraint

$$b_i = b(\boldsymbol{u}_i) = \boldsymbol{u}_i^T \boldsymbol{M}\boldsymbol{u}_i - 1 = 0, \qquad i = 1,\ldots,l, \tag{3}$$

where $\boldsymbol{u}_i$ is the i^{th} eigenvector.

Inverse Problem Formulation

We consider the general discretized PDE-constrained optimization problem

$$\begin{aligned} \underset{\{\lambda_i\},\{\boldsymbol{u}_i\},\boldsymbol{p}}{\text{minimize}} \quad & J(\{\lambda_i\}, \{\boldsymbol{u}_i\}, \boldsymbol{p}) \\ \text{subject to} \quad & \boldsymbol{g}(\lambda_i, \boldsymbol{u}_i, \boldsymbol{p}) = \boldsymbol{0}, \quad i = 1,\ldots,l, \\ & b(u_i) = 0, \quad i = 1,\ldots,l, \\ & \underline{\boldsymbol{p}} \leq \boldsymbol{p} \leq \overline{\boldsymbol{p}}, \end{aligned}$$

where $\boldsymbol{p} \in \mathbb{R}^n$ is the parameter vector, $\underline{\boldsymbol{p}} \in \mathbb{R}^n$ and $\overline{\boldsymbol{p}} \in \mathbb{R}^n$, $\underline{\boldsymbol{p}} \leq \overline{\boldsymbol{p}}$, are the vectors of elementwise lower and upper bounds, respectively, $J : \mathbb{R}^l \times \mathbb{R}^k \times \mathbb{R}^n \to \mathbb{R}$ is the cost function and $\boldsymbol{g} : \mathbb{R} \times \mathbb{R}^m \times \mathbb{R}^n \to \mathbb{R}^m$ and $b : \mathbb{R}^m \to \mathbb{R}$ represent the discretized constraint equations.

The objective function for the eigenvalue problem depends on the eigenvalues, eigenvectors, and parameters. Given a set of experimentally measured eigenvalues $\{\lambda_{mi}\}$, and corresponding experimentally measured eigenvectors $\{\boldsymbol{u}_{mi}\}$, we have

$$J(\{\lambda_i\}, \{\boldsymbol{u}_i\}, \boldsymbol{p}) := \frac{\beta_i}{2}\|\{r_i\}\|^2 + \frac{\kappa_i}{2}\mathscr{G}(\{\boldsymbol{u}_i\}, \{\boldsymbol{u}_{mi}\}) + \mathscr{R}(\boldsymbol{p}), \tag{4}$$

where the $r_i = \frac{\lambda_i - \lambda_{mi}}{\lambda_{mi}}$ represents the relative misfit in the i^{th} eigenvalue, $\|\{r_i\}\|$ represents the Euclidean norm in $\mathbb{R}^l$, $\mathscr{G} : \mathbb{R}^k \times \mathbb{R}^k \to \mathbb{R}$ is a functional that measures the misfit in the eigenmodes, β_i and κ_i are vectors of scaling constants and $\mathscr{R} : \mathbb{R}^n \to \mathbb{R}$ is a regularization operator. Note that β_i and κ_i can be used to specify the relative importance of the individual modes in the optimization problem, as well as turn modes on or off, in the event that there are missing modes in the experimental data. An interesting special case is to consider only the first term in the objective function. In that case, the objective depends only on the eigenvalues, and we have

$$J(\{\lambda_i\}, \boldsymbol{p}) := \frac{1}{2}\|\{r_i\}\|^2 + \mathscr{R}(\boldsymbol{p}). \tag{5}$$

We assume that the system has no zero energy modes, i.e., $\lambda_{mi} \neq 0$ for $i = 1, \ldots, l$.

To solve this problem numerically, we minimize the reduced objective, see,[12]

$$\widehat{J}(\boldsymbol{p}) := J(\boldsymbol{\lambda}(\boldsymbol{p}), \boldsymbol{u}(\boldsymbol{p}), \boldsymbol{p}),$$

where under suitable assumptions $(\boldsymbol{\lambda}(\boldsymbol{p}), \boldsymbol{u}(\boldsymbol{p}))$ solve the original eigenvalue problem for a fixed parameter $\boldsymbol{p}$, subject to the bound constraints, i.e.,

$$\underset{\boldsymbol{p}}{\text{minimize}} \;\; \widehat{J}(\boldsymbol{p}) \quad \text{subject to} \quad \underline{\boldsymbol{p}} \leq \boldsymbol{p} \leq \overline{\boldsymbol{p}}. \tag{6}$$

The first-order necessary optimality conditions for (6) are: if $\boldsymbol{p}$ solves (6) then the compoments of $\boldsymbol{p}$ satisfy

$$\boldsymbol{p}_j = \begin{cases} \underline{\boldsymbol{p}}_j & \text{if } \nabla\widehat{J}(\boldsymbol{p})_j > 0 \\ \boldsymbol{p}_j & \text{if } \nabla\widehat{J}(\boldsymbol{p})_j = 0 \\ \overline{\boldsymbol{p}}_j & \text{if } \nabla\widehat{J}(\boldsymbol{p})_j < 0 \end{cases}$$

or succinctly

$$\boldsymbol{p} = \max\{\underline{\boldsymbol{p}}, \min\{\overline{\boldsymbol{p}}, \boldsymbol{p} - c\nabla\widehat{J}(\boldsymbol{p})\}\} \quad \text{for fixed } c > 0. \tag{7}$$

To compute the gradient of $\widehat{J}$, we define the Lagrangian functional

$$\mathscr{L}(\boldsymbol{u}, \boldsymbol{\lambda}, \boldsymbol{p}, \boldsymbol{w}, \boldsymbol{\eta}) := J + \sum_{i=i}^{n} \left\{ \boldsymbol{w}_i^T \boldsymbol{g}_i + \eta_i b_i \right\}, \tag{8}$$

where $\boldsymbol{w} = \{\boldsymbol{w}_i\}$ is the Lagrange multiplier corresponding to the PDE operator $\boldsymbol{g}$, and η_i is the Lagrange multiplier corresponding to the orthonormality constraint b_i. The gradient of the Lagrangian is given by

$$\begin{Bmatrix} \mathscr{L}_{\lambda_i} \\ \mathscr{L}_{\boldsymbol{u}_i} \\ \mathscr{L}_{\boldsymbol{p}} \\ \mathscr{L}_{\boldsymbol{w}_i} \\ \mathscr{L}_{\eta_i} \end{Bmatrix} = \begin{Bmatrix} J_{\lambda_i} - \boldsymbol{u}_i^T \boldsymbol{M} \boldsymbol{w}_i \\ J_{\boldsymbol{u}_i} + \boldsymbol{g}_{\boldsymbol{u}_i}{}^T \boldsymbol{w}_i + b_{\boldsymbol{u}_i}\eta_i \\ J_{\boldsymbol{p}} + \boldsymbol{g}_{\boldsymbol{p}}^T \boldsymbol{w} \\ \boldsymbol{g}_i \\ b_{\boldsymbol{u}_i} \end{Bmatrix}, \tag{9}$$

where $i = 1, \ldots, l$, $J_{\boldsymbol{u}_i} = \mathscr{G}_{\boldsymbol{u}_i}$ is the derivative of the objective function with respect to the state variables, $J_{\boldsymbol{p}}$ is the derivative with respect to the design parameters, etc. We note that the eigenvalue

solver in Sierra-SD computes mass-normalized modes that satisfy the orthonormality constraint. Thus, the solution of the forward problem could be thought of as satisfying the conditions on both $\boldsymbol{g}_i$ and equation (3), i.e.

$$\begin{Bmatrix} \boldsymbol{g}_i \\ b_i \end{Bmatrix} = \{\mathbf{0}\} \tag{10}$$

for $i = 1, \ldots, l$.

To compute the reduced gradient, we first solve the adjoint equations, i.e., the first and second equations in (9). Expanding the second equation in (9) yeilds

$$\boldsymbol{g}_{\boldsymbol{u}_i}{}^T \boldsymbol{w}_i = -J_{\boldsymbol{u}_i} - b_{\boldsymbol{u}_i} \eta_i \tag{11}$$

or, simplifying,

$$(\boldsymbol{K} - \lambda_i \boldsymbol{M}) \boldsymbol{w}_i = -J_{\boldsymbol{u}_i} - \boldsymbol{M}\boldsymbol{u}_i \eta_i. \tag{12}$$

Since the left hand side of equation (12) is simply the original PDE operator, and λ_i is a known eigenvalue, the linear system is singular. In order to ensure that we have a solution, we must make the right hand side orthogonal to the eigenvector $\boldsymbol{u}_i$. Premultiplying the right hand side of equation (12) by $\boldsymbol{u}_i{}^T$, and setting to zero, and using the fact that the modes are orthonormal (equation (3)), we have

$$\eta_i = -\boldsymbol{u}_i^T J_{\boldsymbol{u}_i} = -\boldsymbol{u}_i^T \mathscr{G}_{\boldsymbol{u}_i}. \tag{13}$$

This gives us an explicit expression for η_i, and by using this η_i we assure that we have a solution of equation (12). Combining this with equation (12), we have

$$(\boldsymbol{K} - \lambda_i \boldsymbol{M}) \boldsymbol{w}_i = -J_{\boldsymbol{u}_i} + \boldsymbol{M}\boldsymbol{u}_i \boldsymbol{u}_i^T J_{\boldsymbol{u}_i} = \left[\boldsymbol{M}\boldsymbol{u}_i \boldsymbol{u}_i^T - \boldsymbol{I}\right] J_{\boldsymbol{u}_i} \tag{14}$$

Now that we have assured that equation (12) will have a solution, we see that due to the singularity the solution could be offset by any linear combination of the vectors in the null space. Thus, we consider an orthogonal decomposition of $\boldsymbol{w}_i$

$$\boldsymbol{w}_i = \boldsymbol{w}_{0i} + \gamma_i \boldsymbol{u}_i \tag{15}$$

where $i = 1, \ldots, l$, and $\boldsymbol{w}_{0i}$ is orthogonal to $\boldsymbol{u}_i$ (that is, $\boldsymbol{u}_i^T \boldsymbol{M} \boldsymbol{w}_{0i} = \mathbf{0}$). $\boldsymbol{w}_{0i}$ can be determined by the singular solve of equation (14). We note that in the special case when the objective function does not depend on $\boldsymbol{u}_i$ (recall equation (5)), equation (14) implies that $\boldsymbol{w}_{0i} = 0$. We consider the first equation in (9) to determine γ_i

$$J_{\lambda\, i} - \boldsymbol{u}_i^T \boldsymbol{M} \boldsymbol{w}_i = J_{\lambda\, i} - \boldsymbol{u}_i^T \boldsymbol{M} \gamma_i \boldsymbol{u}_i = 0. \tag{16}$$

This implies that

$$\gamma_i \boldsymbol{u}_i^T M \boldsymbol{u}_i = \gamma_i = J_{\lambda\, i}. \tag{17}$$

Thus, we have found the Lagrange multiplier $\boldsymbol{w}_i$ is simply a scaled version of the eigenvector $\boldsymbol{u}_i$ plus an offset,

$$\boldsymbol{w}_i = \boldsymbol{w}_{0i} + J_{\lambda\, i} \boldsymbol{u}_i. \tag{18}$$

Using these result, we can compute a reduced gradient as

$$\nabla \widehat{J}(\boldsymbol{p}) = J_{\boldsymbol{p}} + \boldsymbol{g}_{\boldsymbol{p}}^T \boldsymbol{w}. \tag{19}$$

In the simple case where the objective function is given by equation (5), we have $J_{\boldsymbol{p}} = \mathscr{R}_{\boldsymbol{p}}$ and

$$\boldsymbol{g}_{\boldsymbol{p}}^T \boldsymbol{w} = \sum_{i=1}^{l} \boldsymbol{g}_{i\boldsymbol{p}}^T \boldsymbol{w}_i = \sum_{i=1}^{l} \boldsymbol{u}_i^T \boldsymbol{K}_{\boldsymbol{p}} \boldsymbol{w}_i = \sum_{i=1}^{l} \left\{ \boldsymbol{u}_i^T \boldsymbol{K}_{\boldsymbol{p}} \boldsymbol{w}_{0i} + \boldsymbol{u}_i^T \boldsymbol{K}_{\boldsymbol{p}} J_{\lambda i} \boldsymbol{u}_i \right\} = \sum_{i=1}^{l} J_{\lambda i} \boldsymbol{u}_i^T \boldsymbol{K}_{\boldsymbol{p}} \boldsymbol{u}_i. \tag{20}$$

Note, the last term in equation (20) is the eigenvalue sensitivity premultiplied by the partial derivative of the objective function J with respect to the eigenvalue $\boldsymbol{\lambda}_i$. In the case of simple objective function (5), we have

$$\boldsymbol{g}_{\boldsymbol{p}}^T \boldsymbol{w} = \sum_{i=1}^{l} \frac{\lambda_i - \lambda_{mi}}{(\lambda_{mi})^2} \boldsymbol{u}_i^T \boldsymbol{K}_{\boldsymbol{p}} \boldsymbol{u}_i. \tag{21}$$

Given the reduced gradient (19), a variety of methods from ROL can be used to compute a parameter, $\boldsymbol{p}$, that satisfies the first-order necessary optimality condition (7).

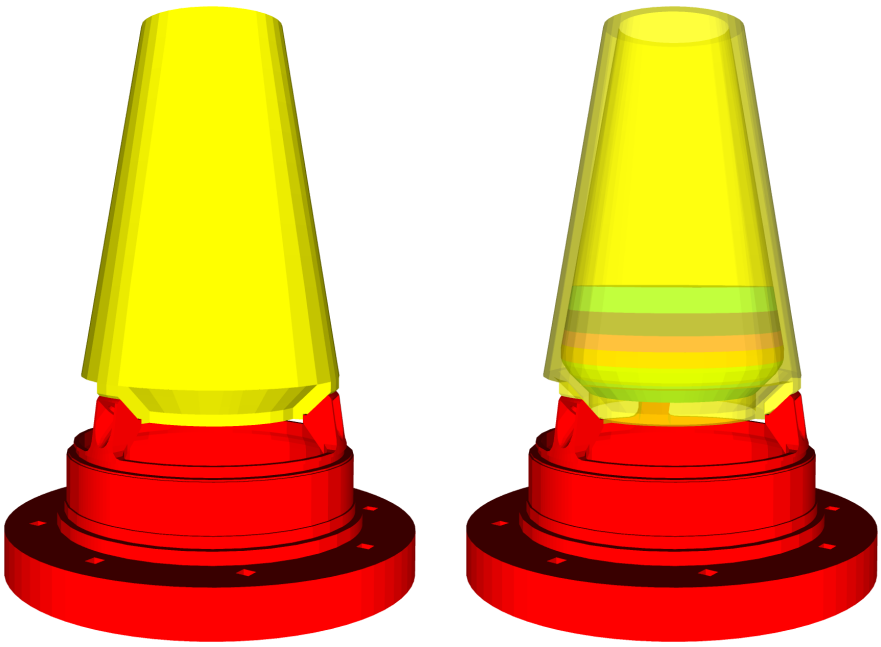

LFU model. View of foam and joint blocks.

Figure 1. LFU model with undetermined joint and foam parameters.

Numerical Results on a LFU Model.

In this section, we present results applying the formulation described in the previous section to the calibration of joint and foam stiffness parameters of a LFU model. This model is shown in Figure 1. The connectors joining the top (yellow) and base (red) are modeled using joint2g elements with unknown stiffness parameters, and the foam blocks are modeled as elastic with unknown bulk and shear moduli.

Inversion with Synthetic Data

A modal analysis of this model was performed in Sierra-SD using the parameters for the joint and foam stiffnesses shown in Tables 1, 2, 3 and 4. The given values of the joint stiffnesses, and bulk/shear moduli of the foams were used to generate a set of synthetic modes/eigenvalues. Then the inverse problem was solved using parameters that had those initial guesses for both the joint and foam parameters. As shown, the initial guesses were chosen to be an order or magnitude smaller than the exact values. This provided a challenging initial guess for the inversion process.

We note the importance of using bound constraints in the optimization procedure, as described in the previous section. Without the bound constraints, the joint stiffness and elastic moduli became negative in certain iterations of the optimization solution. This caused failures in the linear solver due to ill-conditioning of the matrices. Table 5 shows the bound constraints used for the parameters involved in the optimization. Tighter bounds resulted in fewer iterations needed to converge the optimization problem.

Tables 1, 2, and 3 show the initial guess, exact, and computed joint2g stiffnesses for the three connecting joints from LFU model, and Table 4 shows the computed bulk and shear moduli of the foams. The computed parameters from the inverse problem were obtained by running 20 iterations of the projected line-search limited-memory BFGS algorithm implemented in ROL.[13] As can be seen, 20 iterations is sufficient to achieve convergence to the desired joint and foam stiffnesses.

Figure 2 shows the convergence of the objective function and gradient as a function of the iteration count. Figures 3 and 4 show the convergence of the objective and gradient, respectively, for cases where bound constraints and design variable scaling were turned on and off. As can be seen, bound constraints and design variable scaling have a significant impact on the objective function convergence. In particular, the objective and relative change in gradient are more pronounced when both bound constraints and design variable scaling are utilized. Without bounds or design variable scaling, Figure 4 shows that the gradient shows little change in 25 iterations. When adding bound constraints, the gradient goes down about 5 orders of magnitude in 25 iterations, and when utilizing both bound constraints and design variable scaling, the gradient drops 7 orders of magnitude. Similar improvements are seen in the objective function results (Figure 3).

Table 1. Joint2G parameters for joint 1 of LFU model.

	kx	ky	kz	krz	kry	krz
exact	2.46e6	2.0e8	2.0e8	N/A	N/A	N/A
computed	2.47e6	2.0e8	2.0e8	N/A	N/A	N/A
initial guess	2.46e5	2.0e8	2.0e8	N/A	N/A	N/A

Table 2. Joint2G parameters for joint 2 of LFU model.

	kx	ky	kz	krz	kry	krz
exact	2.46e6	2.0e8	2.0e8	N/A	N/A	N/A
computed	2.47e6	2.0e8	2.0e8	N/A	N/A	N/A
initial guess	2.46e5	2.0e8	2.0e8	N/A	N/A	N/A

Inversion with Experimental Data

In this section, we present material inversion results on the LFU model using actual experimental modal data. Two top and three base units were combined into 6 separate realizations of LFU

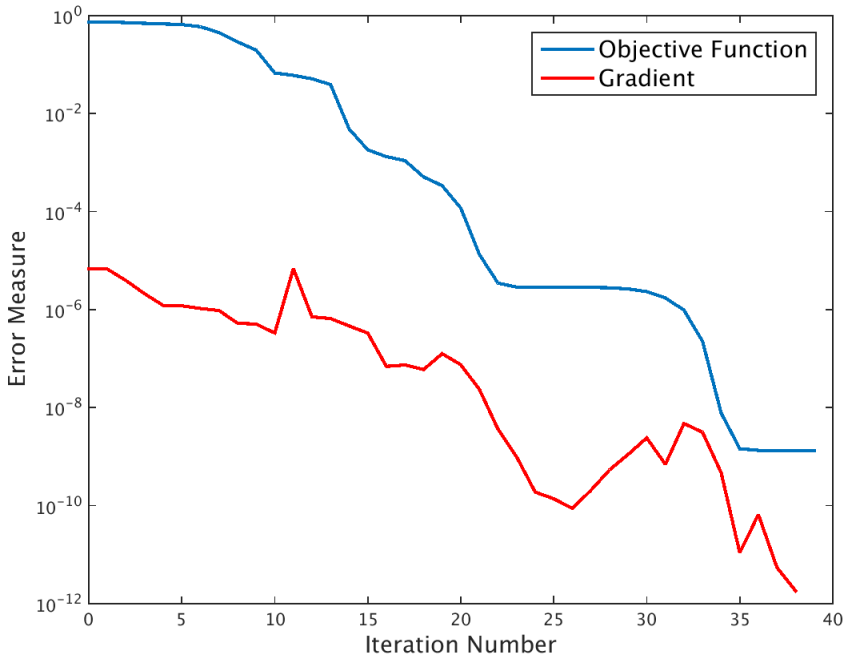

Figure 2. Convergence of objective function and gradient with iteration count.

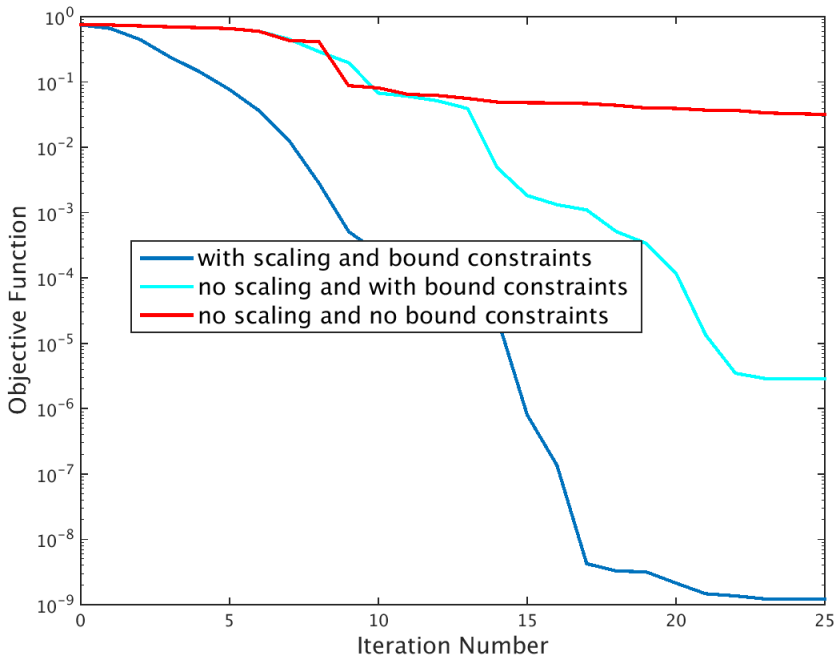

Figure 3. Convergence of objective function with and without bound constraints and design variable scaling.

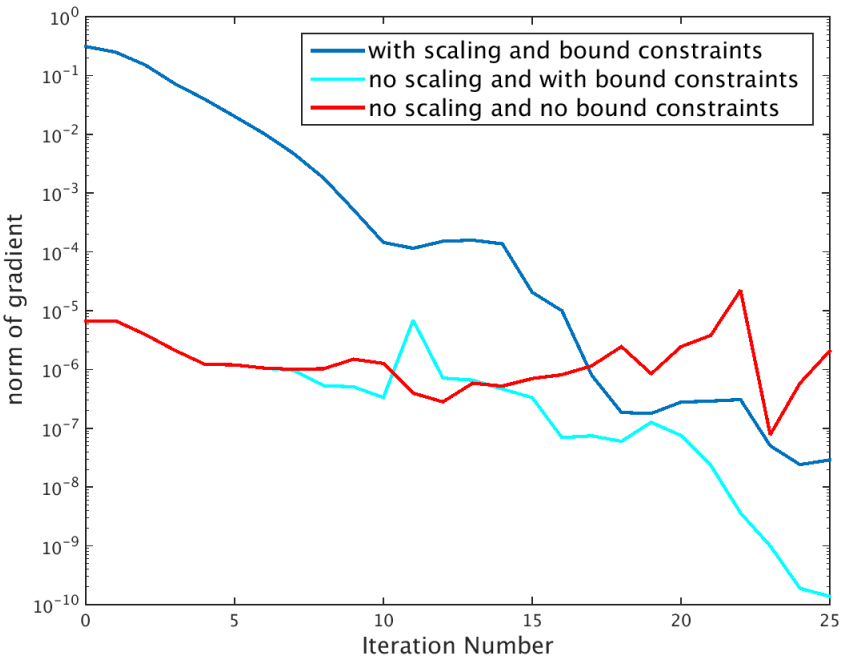

Figure 4. Convergence of gradient with and without bound constraints and design variable scaling.

Table 3. Spring parameters for joint 3 of LFU model.

	kx	ky	kz	krz	kry	krz
exact	2.46e6	2.0e8	2.0e8	N/A	N/A	N/A
computed	2.47e6	2.0e8	2.0e8	N/A	N/A	N/A
initial guess	2.46e5	2.0e8	2.0e8	N/A	N/A	N/A

Table 4. Elastic foam parameters for LFU model.

	shear modulus (G)	bulk modulus (K)
exact	1.585e4	4.134e4
computed	1.585e4	4.134e4
initial guess	1.585e3	4.134e3

models, each of which was disassembled and reassembled 3 times, yielding a total of eighteen realizations of the model. Modal tests were performed on each model, and the first two axial modes were extracted from each model. The average axial frequencies from all eighteen tests are given in Table 6.

The modes given in Table 6 were used as input to the material inverse problem, wherein the unknown parameters were the axial stiffnesses (i.e. in the x direction) of the three joint2g elements, and the bulk/shear modulus of the foam. The modal frequencies and predicted stiffness parameters from the inversion are given in Tables 7 and 8, respectively. Similar curves as given in Figures 3 and 4 were observed during the optimization, with relative change in objective and gradient exceeding $1e^{-10}$.

Various initial guesses for the joint2g and foam stiffnesses were assumed, ranging from an order of magnitude above and below the converged values. It was found that by changing initial guess, the joint2g stiffnesses and shear modulus of the foam converged to about the same values, but the bulk modulus of the foam varied with initial guess. Thus, it is likely that additional modes are needed to accurately characterize the foam bulk modulus.

Finally, we note that 18 sets of modes were measured, but since we are only inverting based on the average of the 18 sets, we only hope to approximate the average properties of the joint and foam stiffnesses. A more interesting study would be to invert each measured set of modes independently to obtain a distribution of material properties. However, given the lack of apparent sensitivity of the measured modes to the bulk modulus, more measurements would be needed to make such a study worthwhile.

Table 5. Bound constraints on parameters for LFU model.

parameter	lower bound	exact	upper bound
G	1.0e3	1.585e4	3.0e5
K	2.0e3	4.134e4	6.0e5
kx	2.0e5	2.46e6	1.0e9
ky	2.0e5	2.46e6	1.0e9
kz	2.0e5	2.46e6	1.0e9

Table 6. Average measured axial modes for the LFU model.

axial mode number	frequency (Hz)
1	1195.0
2	2085.0

Table 7. Comparison of average measured and predicted axial modes for the LFU model.

axial mode number	measured frequency (Hz)	predicted frequency (Hz)
1	1195.0	1195.0
2	2085.0	2085.0

Table 8. Predicted stiffness parameters for the LFU model.

kx	2.72e6
foam shear modulus	1.4e4
foam bulk modulus	1.1e4

Conclusions

In this report, we presented an eigenvalue-based material inversion formulation, which we then implemented using Sierra-SD and ROL. For this problem, bound constraints and design variable scaling on the parameters were found to be essential for the solution of the presented numerical examples. We demonstrated a successful calibration of joint and foam stiffness parameters in an LFU model using the projected line-search limited-memory BFGS algorithm in ROL, with both synthetic and actual experimental modal data.

Future work will involve enabling second-order (i.e. Newton-based) methods for eigenvalue optimization, in both reduced and full-space formuations.

References

[1] BHARDWAJ, M.; PIERSON, K.; REESE, G.; WALSH, T.; DAY, D.; ALVIN, K.; PEERY, J.; FARHAT, C. & LESOINNE, M. (2002). Salinas: a scalable software for high-performance structural and solid mechanics simulations. *Supercomputing, ACM/IEEE 2002 Conference*. IEEE. 35–35.

[2] BIEGLER, L. T. (2003). *Large-scale PDE-constrained optimization*. vol. 30. Springer Verlag.

[3] BONNET, M. & CONSTANTINESCU, A. (2005). Inverse Problems in Elasticity. *Inverse Problems 21(1)*: R1–R50.

[4] CHAMOIN, L.; LADEVEZE, P. & WAEYTENS, J. (2014). Goal-Oriented Updating of Mechanical Models Using the Adjoint Framework. *J. Comp. Mech 54*, 6: 1415–1430.

[5] CHU, M. & GOLUB, G. (1998). *Inverse Eigenvalue Problems: Theory, Algorithms, and Applications*. Oxford Science.

[6] CHU, M. & GOLUB, G. (2002). Structured Inverse Eigenvalue Problems. *Acta Numerica 11*: 1–71.

[7] DOHRMANN, C.. (1998). Draft User's Manual for PESTDY.
Internal Memorandum.

[8] ELDRED, M.; VENKAYYA, V. & ANDERSON, W. (1994). Mode Tracking Issues in Aeroelastic Analysis. Tech. Rep. SAND94-0602J. Sandia National Laboratories.

[9] ENGINEERING, A.. (). Attune User's Guide.

[10] HEROUX, M.; BARTLETT, R.; HOWLE, V.; HOEKSTRA, R.; J., H.; KOLDA, T.; LEHOUCQ, R.; LONG, K.; PAWLOWSKI, R.; PHIPPS, E.; SALINGER, A.; THORNQUIST, H.; TUMINARO, R.; WILLENBRING, J.; WILLIAMS, A. & STANLEY, K. (2005). An overview of the Trilinos project. *ACM Trans. Math. Softw. 31*, 3: 397–423.

[11] HINZE, M.; PINNAU, R.; ULBRICH, M. & ULBRICH, S. (2009). *Optimization with PDE Constraints*. vol. Mathematical Modeling: Theory and Applications, 23. Springer Verlag.

[12] JOHNSON, S. G. (2012). Notes on Adjoint Methods. *Lecture notes, Massachusetts Institute of Technology*.

[13] KOURI, D. P.; RIDZAL, D.; VAN BLOEMEN WAANDERS, B. G. & VON WINCKEL, G.. (2014). Rapid Optimization Library, SAND2014-19572 C, Sandia National Laboratories, https://trilinos.org/packages/rol.

[14] NOCEDAL, J. & WRIGHT, S. (2006). *Numerical Optimization*. Springer.

[15] OBERAI, A.; GOKHALE, N. & FEIJOO, G. (2003). Solution of Inverse Problems in Elasticity Imaging Using the Adjoint Method. *Inverse Problems 19(2)*: 297–313.

[16] RACHOWICZ, W. & ZDUNEK, A. (2011). Application of the FEM with Adaptivity for Electromagnetic Inverse Medium Scattering Problems. *Comput. Methods Appl. Mech. Engrg. 200*: 2337–2347.

[17] REESE, G. (1993). Parameter Estimation Using Genetic Algorithms. Tech. Rep. SAND93-1298C. Sandia National Laboratories.

[18] REESE, G.; BHARDWAJ, M. & WALSH, T. (2009). Salinas- Theory Manual. Tech. Rep. SAND2009-0748. Sandia National Laboratories.

[19] SCHRAMM, H. & ZOWE, J. (1992). A Version of the Bundle Idea for Minimizing a Nonsmooth Function: Conceptual Idea, Convergence Analysis, Numerical Results. *SIAM J. Optimization 2*, 1: 121–152.

[20] SEYRANIAN, A.; LUND, E. & OLHOFF, N. (1994). Multiple Eigenvalues in Structural Optimization Problems. *Structural Optimization 8*: 207–227.

[21] WALSH, T.; AQUINO, W.; RIDZAL, D.; KOURI, D. & VAN BLOEMENN WAANDERS, B. (2014). Viscoelastic Material Inversion using SIERRA/SD and ROL. Tech. Rep. SAND2014-19498. Sandia National Laboratories.

[22] WALSH, T.; AQUINO, W. & ROSS, M. (2013). Source Identification in Acoustics and Structural Mechanics using SIERRA/SD. Tech. Rep. SAND2013-2689. Sandia National Laboratories.

DISTRIBUTION:

2	MS 9018	Central Technical Files, 8945-1
2	MS 0899	Technical Library, 9616

This page intentionally left blank.

Sandia National Laboratories